

An Idiosyncrasy of Time-discretization in Reinforcement Learning

Kris De Asis

kldeasis@ualberta.ca

Department of Computing Science

University of Alberta

Richard S. Sutton

rsutton@ualberta.ca

Department of Computing Science

University of Alberta

Abstract

Many reinforcement learning algorithms are built on an assumption that an agent interacts with an environment over fixed-duration, discrete time steps. However, physical systems are continuous in time, requiring a choice of time-discretization granularity when digitally controlling them. Furthermore, such systems do not wait for decisions to be made before advancing the environment state, necessitating the study of how the choice of discretization may affect a reinforcement learning algorithm. In this work, we consider the relationship between the definitions of the continuous-time and discrete-time returns. Specifically, we acknowledge an idiosyncrasy with naively applying a discrete-time algorithm to a discretized continuous-time environment, and note how a simple modification can better align the return definitions. This observation is of practical consideration when dealing with environments where time-discretization granularity is a choice, or situations where such granularity is inherently stochastic.

1 Introduction

Reinforcement learning provides a framework for solving sequential decision making problems based on evaluative feedback (Sutton & Barto, 2018). It remains a promising approach for robot learning as it can allow for real-time adaptation of behavior. Many reinforcement learning algorithms assume that the agent-environment interaction occurs at synchronous, discrete time steps, where the environment waits for an action before advancing. In contrast, real-world physical systems are continuous in time, and do not wait for an agent’s input. As such, time-discretization becomes a necessary and important consideration (Mahmood et al., 2018a).

Prior work suggests that current reinforcement learning algorithms are sensitive to the choice of discretization. Tallec et al. (2019) emphasizes that action-values converge to state-values as the discretization interval approaches zero, creating degenerate cases for algorithms like Q-learning. Similarly, Munos (2006) shows that the variance of policy gradients can explode under the same limit. Mahmood et al. (2018a) details the trade-off between having fine-grained control and being able to discern the changes between subsequent states. Finally, Farrahi & Mahmood (2023) provides guidelines for time-discretization-aware parameter selection by acknowledging how changes in discrete-time parameters influence the underlying continuous-time objective.

In this work, we explicitly view the discrete-time objective as a discrete approximation of the continuous-time objective. By considering *when* rewards occur, particularly in existing continuous-control environment setups, we identify an idiosyncratic dependence on the choice of discretization beyond those listed in Tallec et al. (2019) and Farrahi & Mahmood (2023). Specifically, the discrete-time return can be viewed as a mixture of two Riemann sums. We characterize and demonstrate that this is a relatively poor integral approximation in comparison with a conventional Riemann sum, and provide a simple modification to the definition of the return to better align the objectives.

The contributions of this work are as follows:

- Acknowledgement and characterization of a discrepancy when naively applying a discrete-time reinforcement learning algorithm to a *discretized* continuous-time environment.
- A simple modification to the definition of the return to avoid a nuanced dependence on time-discretization, based on an integral approximation perspective.
- Characterization of when the modification is most impactful, supported by empirical results demonstrating improved alignment with an underlying continuous time objective.

2 Definitions of the Return

Reinforcement learning (Sutton & Barto, 2018) is a framework for sequential decision making from evaluative feedback. A learning system, denoted an agent, observes its current situation and selects an action, after which it observes a new situation while receiving a reward. The agent’s objective is to learn to act so as to maximize its expected *return*- a discounted sum of future rewards. In discrete-time (Sutton & Barto, 2018), the return from a time step t onward is defined to be:

$$\check{G}_t = \sum_{k=t}^{T-1} \gamma^{k-t} R_{k+1} \quad (1)$$

where T is the final time step in an episodic task, or ∞ in a continuing, infinite-horizon one. In continuous-time reinforcement learning (Doya, 2000; Mehta & Meyn, 2009; Frémaux et al., 2013; Lee & Sutton, 2021; Tallec et al., 2019), we instead define the *integral return* from time step t onward:

$$G_t = \int_t^T \gamma^{\tau-t} R_\tau d\tau \quad (2)$$

Such a formulation is pertinent to applications involving real-time interaction, such as robotics. Despite being continuous in time, they are often digitally controlled, and as such time-discretization becomes a necessary consideration (Mahmood et al., 2018a).

3 When Rewards Occur

There are notation inconsistencies in the literature with respect to time indices in the discrete time return (Equation 1). Some define it to start from R_{t+1} (Sutton, 1988; Precup et al., 2000; van Seijen et al., 2009; Barreto et al., 2017), as presented in this document, while some would start from R_t (Watkins, 1989; van Hasselt, 2010; Mnih et al., 2015; Wang et al., 2016). This inconsistency is inconsequential when solely considering the discrete-time setting, as the rewards occur at the same locations in an agent’s stream of experience. However, it has implications when viewed as a discrete approximation to an underlying integral return. Thus, it is worth considering *when* rewards occur.

We emphasize the focus on a setting where there is an underlying continuous-time objective, of which a digital learning agent samples at an arbitrary (and potentially variable) frequency. Despite the discrete-time notation inconsistencies, it is often agreed upon that from the agent’s perspective, the reward and next state are jointly observed. This is reflected in environment step calls in relatively standard reinforcement learning APIs (Brockman et al., 2016), agent-environment interaction diagrams (Sutton & Barto, 2018), or explicit acknowledgement that reward can be a function of state, action, and *next state* (Puterman, 1994). In real-time settings which do not wait for an agent’s input, actions typically take time to execute and have an influence, and so meaningful evaluative feedback must come *after* time t . Hardware limitations on sampling rates further impose an inherent delay in when a system can receive feedback for an action. In many existing robotics environments, where the considered setting is especially pertinent, rewards are often explicitly computed based on the next time step’s state information (Todorov et al., 2012; Brockman et al., 2016; Mahmood et al., 2018b), for example, rewards based on distance traveled in some direction between two time steps, or distance between an end-effector and a desired setpoint at the subsequent time step.

Of note, semi-MDPs and options (Sutton et al., 1999; Precup, 2000) address the problem of when rewards occur, but under the assumption that one has access to higher-frequency interaction with the environment to integrate the discounted sum of rewards within the discretization interval. It is akin to the agent being aware of and able to time when each component of a temporally-extended reward occurs. In this work, we consider when one does not have access to these higher-frequency samples, but is aware of how much time has elapsed between discrete decision points. Acquiring such information may not be possible due to hardware limitations, and highlights a nuance that arises when *naively* applying a discrete-time algorithm to a discretized continuous-time environment.

4 Implications for Time Discretization

If we consider rewards jointly arriving with the next state, at least from the agent’s perspective, this results in an idiosyncrasy with respect to approximating an underlying integral return. While the discrete-time returns may use inconsistent reward time-indices, they are consistent on when discounting begins: the first reward is given weight $\gamma^0 = 1$, with subsequent rewards weighted by increasing powers of γ . We can view the integral return in Equation 2 to be of the form:

$$\int_t^T f(\tau)g(\tau)d\tau \quad (3)$$

where $f(\tau)$ is the discounting term, and $g(\tau)$ is the reward signal. A right-point Riemann sum approximation to this would yield:

$$\sum_{i=0}^{n-1} f(\tau_i)g(\tau_i)\Delta \quad (4)$$

where $\Delta = \frac{T-t}{n}$ and $\tau = \{t + \Delta, t + 2\Delta, \dots, T\}$. The right-point Riemann sum beginning with $t + \Delta$ aligns with an agent jointly receiving a reward with the observation of the next state. However, this sum would weight the first reward by $\gamma^\Delta \neq \gamma^0$. This highlights that if one naively applies a discrete-time reinforcement learning algorithm to a discretized continuous-time environment, it is akin to a left-point Riemann sum for discounting, and a right-point Riemann sum for rewards:

$$\sum_{i=0}^{n-1} f(\tau_i)g(\tau_{i+1})\Delta \quad (5)$$

where $\tau \in \{t, t + \Delta, t + 2\Delta, \dots, T\}$. See Figure 1 for a visualization of this Riemann sum. This sum still converges to the correct integral as $n \rightarrow \infty$, as Bliss’s Theorem (1914) allows each function to be evaluated at *any point* within the interval. However, for the specific case where a left-point Riemann sum is used for discounting, we expect this to perform *worse* than committing to a right-point Riemann sum. Due to the curvature of exponential decay, if one drew a rectangle with opposite corners at any two points, there will always be more area above the curve than below, implying an underestimate has strictly lower error than an overestimate. This is visualized in Figure 2.

To rectify this discrepancy and commit to a right-point Riemann sum approximation, one would simply multiply the discrete-time return by a factor of γ (assuming $\Delta = 1$):

$$\gamma \ddot{G}_t = \gamma R_{t+1} + \gamma^2 R_{t+2} + \dots \quad (6)$$

For a *fixed, pre-specified* action cycle-time Δ , there is no loss of generality as the discrete-time return is proportional by a factor of $\gamma^\Delta \Delta$. However, this is not the case when Δ may vary over time, e.g., due to an adaptive algorithm (Karimi et al., 2023) or inherent stochasticity. These concerns similarly apply to a variable γ and may extend toward tuning fixed- Δ and/or γ in practice in terms of a nuanced and unintuitive dependence on discretization. See appendix A for a discrete-time return visualization with variable interval sizes. To emphasize the dependence on Δ , we note the explicit

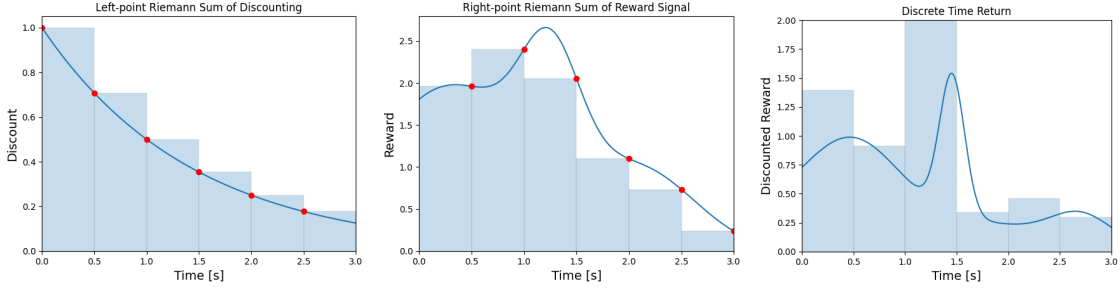


Figure 1: The resulting sum when applying a discrete-time algorithm to a discretized continuous-time domain. Note how rectangle heights may fall out of the function’s range within an interval.

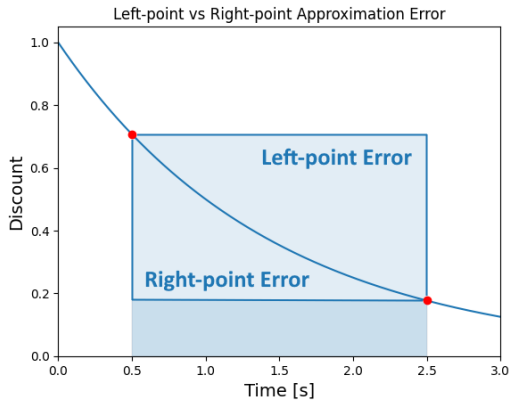


Figure 2: A visualization of the left-point and right-point Riemann sum approximation errors for an exponential decay. Due to curvature, a right-point Riemann sum will always have lower error.

right-point Riemann sum return:

$$\begin{aligned} \ddot{G}_t^{RP} &\stackrel{\text{def}}{=} \sum_{k=t}^{T-1} \gamma^{\sum_{i=t}^k \Delta_{i+1}} R_{k+1} \Delta_{k+1} \\ &= \gamma^{\Delta_{t+1}} R_{t+1} \Delta_{t+1} + \gamma^{\Delta_{t+1} + \Delta_{t+2}} R_{t+2} \Delta_{t+2} + \dots \end{aligned} \quad (7)$$

Prior work has acknowledged the modifications of (1) scaling rewards by Δ , and (2) exponentiating γ by Δ (Tallec et al., 2019; Farrahi & Mahmood, 2023) in improving robustness to time-discretization. The key difference and contribution in Equation 7 being the earlier discounting.

5 Comparison with Standard Riemann Sums

To see how the discrete-time return (DTR) in Equation 5 fares against a right-point Riemann sum, we evaluate them on randomly generated continuous-time signals. Inspired by robotics, we consider periodic signals, and Gaussian mixtures. Periodic signals are comparable to signals pertaining to robot locomotion, while Gaussian mixtures instead resemble both sparse and distance-based rewards, depending on the spread of each Gaussian. We fix the signal length to 3 seconds, with no loss of generality due to being continuous in time. Each signal generator is detailed below:

Random Periodic Signals - This signal sums 6 sinusoids $\sum_{i=0}^5 A_i \sin(\omega_i t + \phi_i)$ with angular frequencies $\omega \in \{\frac{2\pi}{4}, \frac{2\pi}{2}, 2\pi, 4\pi, 8\pi, 16\pi\}$, amplitudes $A_i \sim \mathcal{N}(0, 1)$, and phase shifts $\phi_i \sim \mathcal{U}(0, 2\pi)$.

Random Gaussian Mixtures - This signal sums 6 Gaussians $\sum_{i=0}^5 \mathcal{N}(\mu_i, \sigma_i)$ with means $\mu_i \sim \mathcal{U}(0, 3)$, and standard deviations $\sigma_i \sim \mathcal{U}(0, \frac{3}{2})$.

For each method, we varied the number of intervals $n \in \{5, 10, 25, 50, 100\}$, the discount factor $\gamma \in \{0.5, 0.75, 0.875\}$, and measured the absolute error of the integral approximation- compared against a mid-point Riemann sum with 10^4 intervals. The values of γ used may appear small and unrepresentative of typical values. We however note that the discount is *per second*, and that for a robot sampling every 30 ms, $\gamma = 0.5$ is effectively $\gamma^\Delta = 0.5^{0.03} \approx 0.98$ per discrete time step. Averaged across 10^6 randomly generated signals of each type, the results can be seen in Figure 3.

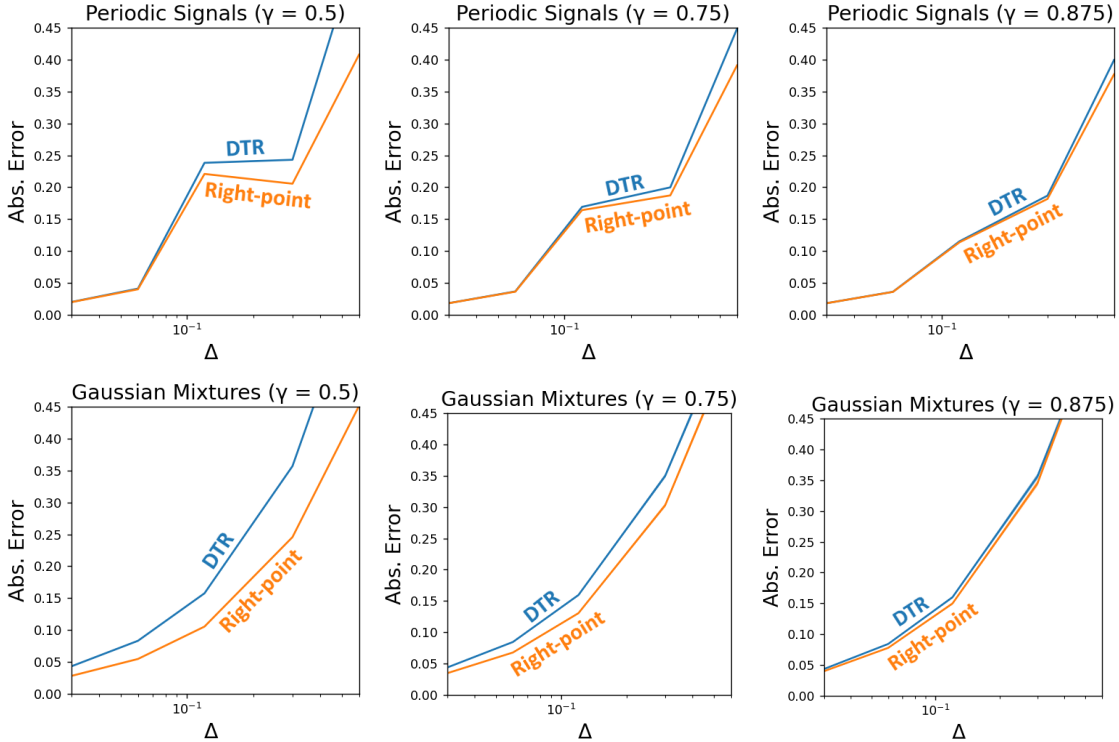


Figure 3: Numerical integration approximation error on *discounted* random signals. Results are averaged over 10^6 signals and shaded regions represent one standard error.

As expected, the errors generally increase as $\Delta \propto \frac{1}{n}$ increases. There’s a consistent dip in error with the periodic signals, likely due to the intervals coincidentally aligning with the pre-specified frequencies. Across all settings, DTR had larger absolute error, consistent with our hypothesis that DTR would perform worse than right-point on discounted signals. The gap closes as $\gamma \rightarrow 1$, as the sums are equivalent at this extreme.

We then considered stochastic intervals to simulate variable time-discretization. This was implemented by sampling, sorting, and re-scaling a set of $n + 1$ uniform random points representing interval endpoints. This is particularly pertinent as DTR is no longer proportional to right-point, and reflects the variability in applications on real-time systems. Fixing $\gamma = 0.75$, Figure 4 shows results averaged across 10^6 randomly generated signals of each type, plotted against *average* Δ . Errors generally increased, with DTR maintaining larger approximation error across every setting.

Lastly, to see whether results hold beyond exponential discounting, we considered the product of each pair of the signal generators. This evaluates each sum in a more general numerical integration setting, while having implications for variable, transition-dependent γ in reinforcement learning. Averaged across 10^6 randomly generated signal pairs, the results can be seen in Figure 5. Perhaps surprisingly, the gap between DTR and the right-point Riemann sum widens dramatically. These results suggest that beyond the structure of discounting, DTR is a generally worse integral approximation.

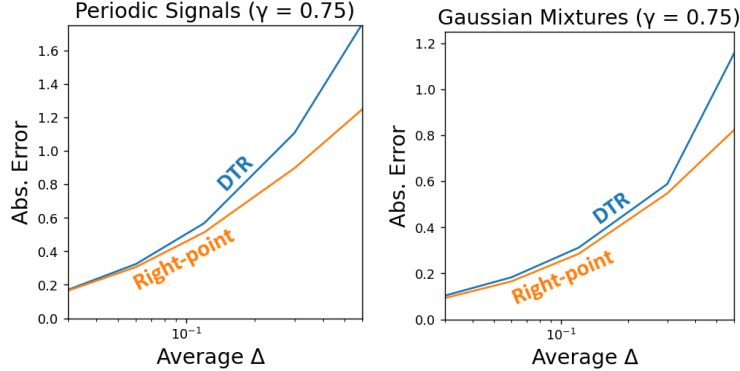


Figure 4: Numerical integration approximation error on *discounted* random signals, with *stochastic discretization intervals*. Results are averaged over 10^6 signals and shaded regions represent one standard error.

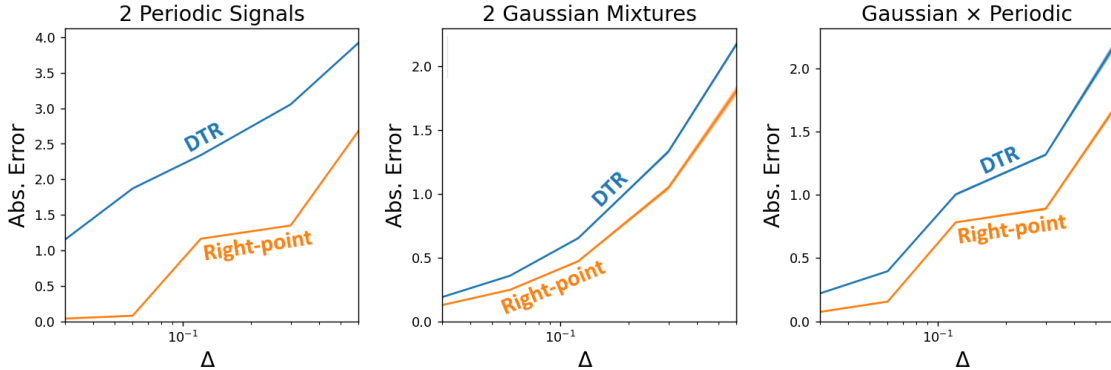


Figure 5: Numerical integration approximation error on *undiscounted* products of random signals. Results are averaged over 10^6 signals and shaded regions represent one standard error.

A key takeaway from these results is that shifting the discount factor in the discrete-time return yields a better prediction target (e.g., in value-based methods) in terms of error between the integral return. To reiterate, in the *fixed* Δ case, the sums are proportional despite the gaps in approximation error. This suggests that the improvement is inconsequential for control. However, such improved alignment is expected to improve control performance in the *variable* Δ setting, in terms of maximizing the underlying integral return. We explore this further in the next section.

6 Discretized Continuous-time Control

To evaluate the right-point Riemann sum in a continuous-time control setting, we build off of the REINFORCE (Williams, 1992) algorithm. Such a choice is due to the algorithm’s simplicity, allowing for more confidence in attributing differences in performance. We specifically use *online* REINFORCE with eligibility traces (Kimura et al., 1995) and dropped γ^t term, summarized by:

$$\begin{aligned} \mathbf{z} &\leftarrow \mathbf{z} + \nabla_{\theta} \log \pi(A_t | S_t) \\ \theta &\leftarrow \theta + \alpha R_{eff} \mathbf{z} \\ \mathbf{z} &\leftarrow \gamma^{\Delta_{t+1}} \mathbf{z} \end{aligned}$$

where Δ_{t+1} is the elapsed time between time steps t and $t + 1$, $R_{eff} = R_{t+1} \Delta_{t+1}$ for the discrete-time return, and $R_{eff} = \gamma^{\Delta_{t+1}} R_{t+1} \Delta_{t+1}$ for the right-point Riemann sum. The above algorithm

employs the recommendations of (Farrahi & Mahmood, 2023) for making algorithms more robust to time-discretization, emphasizing that the proposed right-point modification is complimentary. Each agent’s policy used a two-hidden-layer fully-connected network with *tanh* activations, with its output being treated as the mean of a Gaussian with an initial (bias unit) standard deviation of 1.

We designed a simulated *Servo Reacher* environment based on the setup in Mahmood et al. (2018b), with physical parameters sourced from a Dynamixel MX-28AT data sheet. This custom environment allows for fine-grained computation of the integral return, and flexibility in the discretization intervals an agent can sample at. Full environment specification can be found in Appendix B. To simulate the inherent stochasticity of a real robot, Gaussian noise was added to the target discretization interval, $\Delta_t \sim \mathcal{N}(\Delta_\mu, 10 \text{ ms})$, with a minimum of 1 ms. We additionally included a 1% chance to sample the interval from $\mathcal{N}(1000 \text{ ms}, 10 \text{ ms})$ to simulate “catastrophic” events akin to communication errors.

The environment fixed $\gamma = 0.25$, which when using an interval of 40 ms, corresponds with discrete-time $\gamma^{0.04} \approx 0.95$. We considered target discretization intervals $\Delta_\mu \in \{40, 80, 120\}$ ms with a 4 second time limit, and measured the episodic integral return. Averaged over 100 25-minute runs, Figure 6 shows parameter sensitivity curves, as well as learning curves under the best parameters.

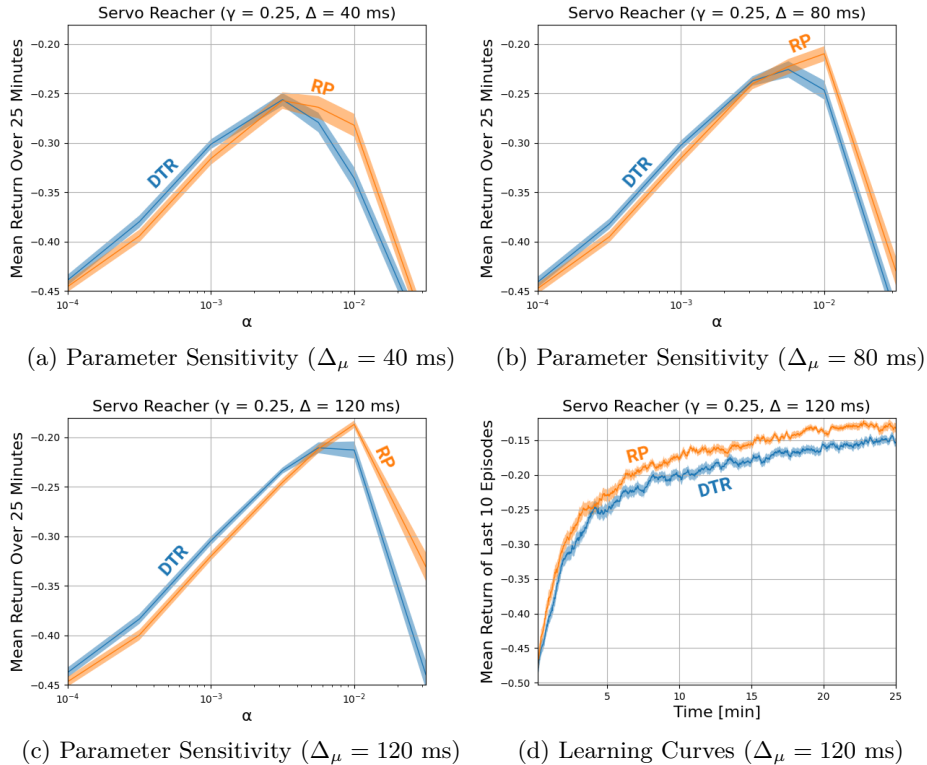


Figure 6: Servo Reacher results for REINFORCE using the discrete-time return (DTR) and right-point Riemann sum (RP), averaged over 100 runs. Shaded regions represent one standard error.

An initial observation is a systematic “lag” between the two algorithms in the sensitivity curves at low α . This is due to the return magnitudes being roughly proportional by a factor of $\mathbb{E}[\gamma^{\Delta_t}]$. If one absorbs this factor into the step-size, the right-point Riemann sum can be viewed as using a smaller *effective* α in the policy gradient update. Scaling the figure to use this effective α can be found to well-align the curves at low α . Nevertheless, we find that after accounting for this shift, REINFORCE with the right-point Riemann sum performs better for large α , and can significantly outperform the discrete-time return with both algorithms properly tuned. The right-point Riemann sum is seen to improve with *increasing* Δ_μ , in line with the approximation error results in Section 5.

Acknowledging that the two returns are roughly proportional by $\mathbb{E}[\gamma^{\Delta t}]$, improvements are expected as this term deviates from 1, i.e., decreasing γ or increasing $\Delta\mu$.

7 Conclusions and Future Work

In this work, we identified and characterized an idiosyncrasy of time-discretization in reinforcement learning. Specifically, a nuance between the definitions of the discrete-time and continuous-time returns when viewing one as a discretization of the other. Our results suggest that when one does not have access to evaluating the integral return via options, one can better align the objectives by shifting the discount factor to begin discounting sooner. This provides *unification* in that the discrete-time return becomes a relatively straight-forward discretization of the integral return. We strongly emphasize the *simplicity* of the modification, and how apart from the $\gamma = 0$ extreme, such a modification has no loss of generality in discrete-time or with fixed discretization intervals due to proportionality with the conventional discrete-time return. The returns are equivalent as $\gamma^{\Delta} \rightarrow 1$, but as it deviates, it results in better prediction targets in terms integral approximation error, and improves control performance with *variable* time-discretization. Beyond the integral approximation perspective, the modification has intuitive appeal in that results from catastrophically long delays are attenuated in the return, rather than fully crediting an action for that outcome.

This work was built on an assumption that the reward better aligns with the subsequent time-step, which is often the case in how existing continuous-time environments are set up. The right-point Riemann sum can be viewed as evaluating the integral within the interval for an *impulse reward* at the subsequent time-step, as would be done by the options framework in a semi-MDP. However, we emphasize that this work still considers problems with arbitrarily dense rewards, but due to discrete sampling, rewards appear as delayed impulse rewards from the agent’s perspective. Should there be additional information about when a reward occurs within an interval, the ideas still generalize in that discounting can be shifted to reflect this information.

Regarding avenues for future work, the integral approximation perspective suggests opportunity to explore return modifications corresponding with other integral approximation techniques. For example, if one were to additionally track predecessor rewards, it opens up the possibility of interpolation-based approximations (e.g., trapezoidal rule). For the case of exponential discounting, we could further leverage a closed-form integral for that term.

Acknowledgements

The authors were generously supported by Amii, NSERC, and CIFAR, and would like to thank Alan Chan and Sungsu Lim for insights and discussions contributing to the results presented in this paper. The authors further thank the reviewers for valuable feedback during the review process.

References

- A. Barreto, W. Dabney, R. Munos, J. J. Hunt, T. Schaul, D. Silver, and H. van Hasselt. Successor features for transfer in reinforcement learning. In *Proceedings of the 30th Annual Conference on Neural Information Processing Systems*, pp. 4055–4065, 2017.
- Gilbert Ames Bliss. A substitute for duhamel’s theorem. *Annals of Mathematics*, 16(1/4):45–49, 1914.
- G. Brockman, V. Cheung, L. Pettersson, J. Schneider, J. Schulman, J. Tang, and W. Zaremba. OpenAI gym. *CoRR*, abs/1606.01540, 2016.
- K. Doya. Reinforcement learning in continuous time and space. *Neural Computation*, 12:219–245, 2000.
- Homayoon Farrahi and A. Rupam Mahmood. Reducing the cost of cycle-time tuning for real-world policy optimization, 2023.

- N. Frémaux, H. Sprekeler, and W. Gerstner. Reinforcement learning using a continuous time actor-critic framework with spiking neurons. *PLOS Computational Biology*, 9:1–21, 2013.
- A. Karimi, J. Jin, J. Luo, A. R. Mahmood, M. Jagersand, and S. Tosatto. Dynamic decision frequency with continuous options, 2023.
- Hajime Kimura, Masayuki Yamamura, and Shigenobu Kobayashi. Reinforcement learning by stochastic hill climbing on discounted reward. In *Proceedings of the 12th International Conference on Machine Learning*, 1995.
- J. Lee and R. S. Sutton. Policy iterations for reinforcement learning problems in continuous time and space — fundamental theory and methods. *Automatica*, 126:109421, 2021. ISSN 0005-1098.
- A. R. Mahmood, D. Korenkevych, B. J. Komer, and J. Bergstra. Setting up a reinforcement learning task with a real-world robot. In *Proceedings of the 2018 IEEE/RSJ International Conference on Intelligent Robots and Systems*, pp. 4635–4640, 2018a.
- A. R. Mahmood, D. Korenkevych, G. Vasan, W. Ma, and J. Bergstra. Benchmarking reinforcement learning algorithms on real-world robots. In *Conference on Robot Learning*, 2018b.
- P. G. Mehta and S. P. Meyn. Q-learning and Pontryagin’s minimum principle. In *Proceedings of the 48th IEEE Conference on Decision and Control. Held jointly with the 2009 28th Chinese Control Conference. CDC/CCC 2009.*, pp. 3598–3605, 2009.
- V. Mnih, K. Kavukcuoglu, D. Silver, A. A. Rusu, J. Veness, M. G. Bellemare, A. Graves, M. A. Riedmiller, A. Fidjeland, G. Ostrovski, S. Petersen, C. Beattie, A. Sadik, I. Antonoglou, H. King, D. Kumaran, D. Wierstra, S. Legg, and D. Hassabis. Human-level control through deep reinforcement learning. *Nature*, 518(7540):529–533, 2015.
- R. Munos. Policy gradient in continuous time. *Journal of Machine Learning Research*, 7:771–791, 2006.
- D. Precup, R. S. Sutton, and S. Singh. Eligibility traces for off-policy policy evaluation. In *Proceedings of the 17th International Conference on Machine Learning, ICML 2000*, pp. 759–766, 2000.
- Doina Precup. *Temporal abstraction in reinforcement learning*. PhD thesis, 2000.
- M. L. Puterman. *Markov Decision Processes: Discrete Stochastic Dynamic Programming*. John Wiley & Sons, Inc., USA, 1st edition, 1994. ISBN 0471619779.
- R. S. Sutton. Learning to predict by the methods of temporal differences. *Machine Learning*, 3: 9–44, 1988.
- R. S. Sutton and A. G Barto. *Reinforcement learning: An introduction*. MIT press, 2018.
- Richard S. Sutton, Doina Precup, and Satinder Singh. Between mdps and semi-mdps: A framework for temporal abstraction in reinforcement learning. *Artificial Intelligence*, 112(1):181–211, 1999. ISSN 0004-3702.
- C. Tallec, L. Blier, and Y. Ollivier. Making deep q-learning methods robust to time discretization. In *Proceedings of the 36th International Conference on Machine Learning*, volume 97, pp. 6096–6104, 2019.
- E. Todorov, T. Erez, and Y. Tassa. Mujoco: A physics engine for model-based control. In *IROS*, pp. 5026–5033. IEEE, 2012.
- H. van Hasselt. Double q-learning. In *Advances in Neural Information Processing Systems*, 2010.

- H. van Seijen, H. van Hasselt, S. Whiteson, and M. A. Wiering. A theoretical and empirical analysis of expected sarsa. In *IEEE Symposium on Adaptive Dynamic Programming and Reinforcement Learning, ADPRL 2009*, pp. 177–184, 2009.
- Z. Wang, T. Schaul, M. Hessel, H. van Hasselt, M. Lanctot, and N. de Freitas. Dueling network architectures for deep reinforcement learning. In *Proceedings of the 33rd International Conference on Machine Learning, ICML 2016*, pp. 1995–2003, 2016.
- C. J. C. H. Watkins. *Learning from Delayed Rewards*. PhD thesis, King’s College, 1989.
- Ronald J Williams. Simple statistical gradient-following algorithms for connectionist reinforcement learning. *Machine Learning*, 8(3-4):229–256, 1992.

A Discrete-time Return Visualization with Variable Interval Sizes

Below we provide a visualization akin to Figure 1, but with variable discretization intervals.

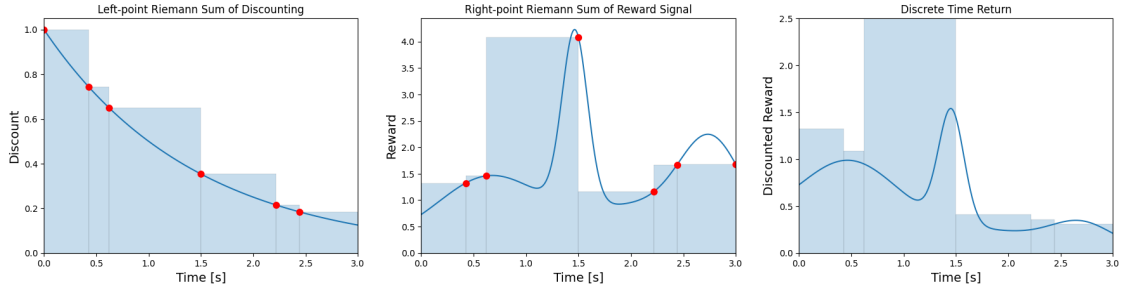


Figure 7: The resulting sum when applying a discrete-time algorithm to a discretized continuous-time domain with variable interval sizes. Note how rectangle heights may fall out of the function’s range within an interval.

B Servo Reacher Environment Details

The environment state \mathbf{x} is a column vector containing the DC motor’s angular velocity [rad/s], the DC motor’s current [A], the output shaft’s angle [rad], the output shaft’s angular velocity [rad/s], and the output shaft’s target angle [rad], respectively. The state vector is updated as follows:

$$\dot{\mathbf{x}}_t \leftarrow \begin{bmatrix} -\frac{b_m}{J_m} & \frac{K_t}{J_m} & 0 & 0 & 0 \\ -\frac{K_t}{L_a} & -\frac{R_a}{L_a} & 0 & 0 & 0 \\ 0 & 0 & 0 & 1 & 0 \\ -\frac{b_m}{J_m N \eta} & \frac{K_t}{J_m N \eta} & 0 & 0 & 0 \\ 0 & 0 & 0 & 0 & 0 \end{bmatrix} \mathbf{x}_t + \begin{bmatrix} 0 \\ \frac{1}{L_a} \\ 0 \\ 0 \\ 0 \end{bmatrix} A_t$$

$$\mathbf{x}_{t+1} \leftarrow \mathbf{x}_t + \dot{\mathbf{x}}_t \Delta_s$$

where $\Delta_s = 10^{-4}$ [s] is the simulation discretization granularity, and A_t is an input voltage with built-in saturation limits of $\in [-12, 12]$ [V]. The output shaft angle is clamped $\in [-1.306, 1.306]$ [rad] in accordance with [Mahmood et al. \(2018b\)](#). The physical parameters used are detailed below:

L_a	Armature Inductance	2.05×10^{-3} [H]
R_a	Armature Resistance	8.29 [Ohm]
J_m	Rotor Inertia	8.67×10^{-8} [kg · m ²]
b_m	Rotor Friction	8.87×10^{-8} [N · m · s]
K_t	Torque Constant	0.0107 [$\frac{\text{N} \cdot \text{m}}{\text{A}}$]
N	Gear Ratio	200
η	Gear Efficiency	0.836

Given a target discretization interval $> 10^{-4}$ [s], the above updates are repeated until the target elapsed time is reached, keeping track of any overshoot and compensating accordingly in the next time interval. As a reinforcement learning environment, an agent observes the output shaft’s angle, angular velocity, and target angle. The initial output shaft angle, θ_0 , and target angle, θ_{target} , are uniformly sampled $\in [-1.306, 1.306]$ at the start of each episode, and an episode terminates when $|\theta_{t+1} - \theta_{target}| < 0.1$ [rad] with angular velocity $\dot{\theta}_{t+1} < 0.1$ [rad/s]. An agent provides a continuous-valued action as a voltage, and receives a reward $|\theta_{t+1} - \theta_{target}|$, computed and received jointly with the next observation.